High Fidelity Reconstructed Attitude Estimation Using Cassini Flight Telemetry†

Thomas A. Burk,*
Jet Propulsion Laboratory, California Institute of Technology, Pasadena, CA, 91109

The Cassini Grand Finale capped the 20 year Cassini mission with 22 one-week-long orbits each with periapsis inside the ring plane just above Saturn's cloud tops. One aspect of these remarkable orbits was unprecedented measurements of Saturn's magnetic field very close to the planet. Processing this data required precise estimates of Cassini's orientation during these ring plane crossings. These periods coincided with planned gyro-only attitude propagation due to the enormous bright bodies in the star tracker field-of-view. This paper describes how attitude reacquisition information, when the star tracker reacquires an absolute inertial reference, can be used to correct errors introduced during gyro-only propagation. The resulting high fidelity reconstruction significantly improves the extraction of Saturn's magnetic field from the raw data obtained during gyro-only periods when Cassini's changing orientation makes precise attitude estimation a challenge.

I. Nomenclature

DSN	=	Deep Space Network (Goldstone, Madrid, Canberra)
FSW	=	Flight Software
HGA	=	High Gain Antenna
HRG	=	Hemispheric Resonator Gyroscope
IRU	=	Inertial Reference Unit
J2000	=	Earth Mean Equator Inertial Frame at January 1, 2000 epoch
MAG	=	Magnetometer
ME	=	Main Engine
ORS	=	Optical Remote Sensing
Rev	=	orbital revolution (Cassini orbit number at Saturn)
RCS	=	Reaction Control System
RWA	=	Reaction Wheel Assembly
S/C	=	Cassini spacecraft
SID	=	Star identification
SRU	=	Steller Reference Unit

II. Introduction

THE Cassini spacecraft finished its epic mission at Saturn on September 15, 2017. After 13 years in Saturn orbit, a carefully planned Titan gravity assist steered the spacecraft into Saturn's atmosphere where it structurally and thermally broke up after transmitting real-time science and engineering data collected during this final "plunge" into Saturn. It was a remarkable end to a 20-year mission of discovery – 13 years in Saturn orbit preceded by a 6.7 year "cruise" through the inner solar system and past Jupiter, reaching Saturn on July 1, 2004. The plunge on September 15th was Cassini's 293rd orbit of Saturn, including 22 Grand Finale orbits[1] with periapsis inside the rings – skimming just above the planet's cloud tops every week between April 26th and the plunge on September 15th. Each of those 22

* Cassini Attitude Control Product Delivery Manager, Guidance and Control Section, M/S 230-104, 4800 Oak Grove Dr., Pasadena, California, 91109, Thomas.A.Burk@jpl.nasa.gov .

orbits included unprecedented science gathering in a region near Saturn where Cassini had never ventured before[2] in its 13-year "tour" of the Saturn system.

Cassini was a 3-axis stabilized spacecraft with an 11-meter magnetometer boom (deployed just before Earth swingby in mid-1999) and three 10-m Radio and Plasma Wave Science antennas. Figure 1 depicts the spacecraft and the spacecraft body axes. The magnetometer booms extends in the +Y direction, the High Gain Antenna (HGA) points in the –Z direction, and the star tracker boresight points in the +X direction. Cassini had co-aligned redundant star trackers, known as stellar reference units (SRUs), with the "prime" unit always on and the backup unit normally powered off. Similarly, Cassini had redundant inertial reference units (IRUs). Cassini's "prime" IRU was always on and the backup IRU was normally powered off. The IRUs were not co-aligned.

Cassini used three orthogonal reaction wheel assemblies (RWAs) for precise pointing control most of the time at Saturn[3]. When not in RWA control, eight thrusters were used in reaction control system (RCS) mode. RCS control used hydrazine in a bang-off-bang control approach. RCS mode permitted slews at higher body rates than were allowed in RWA control.

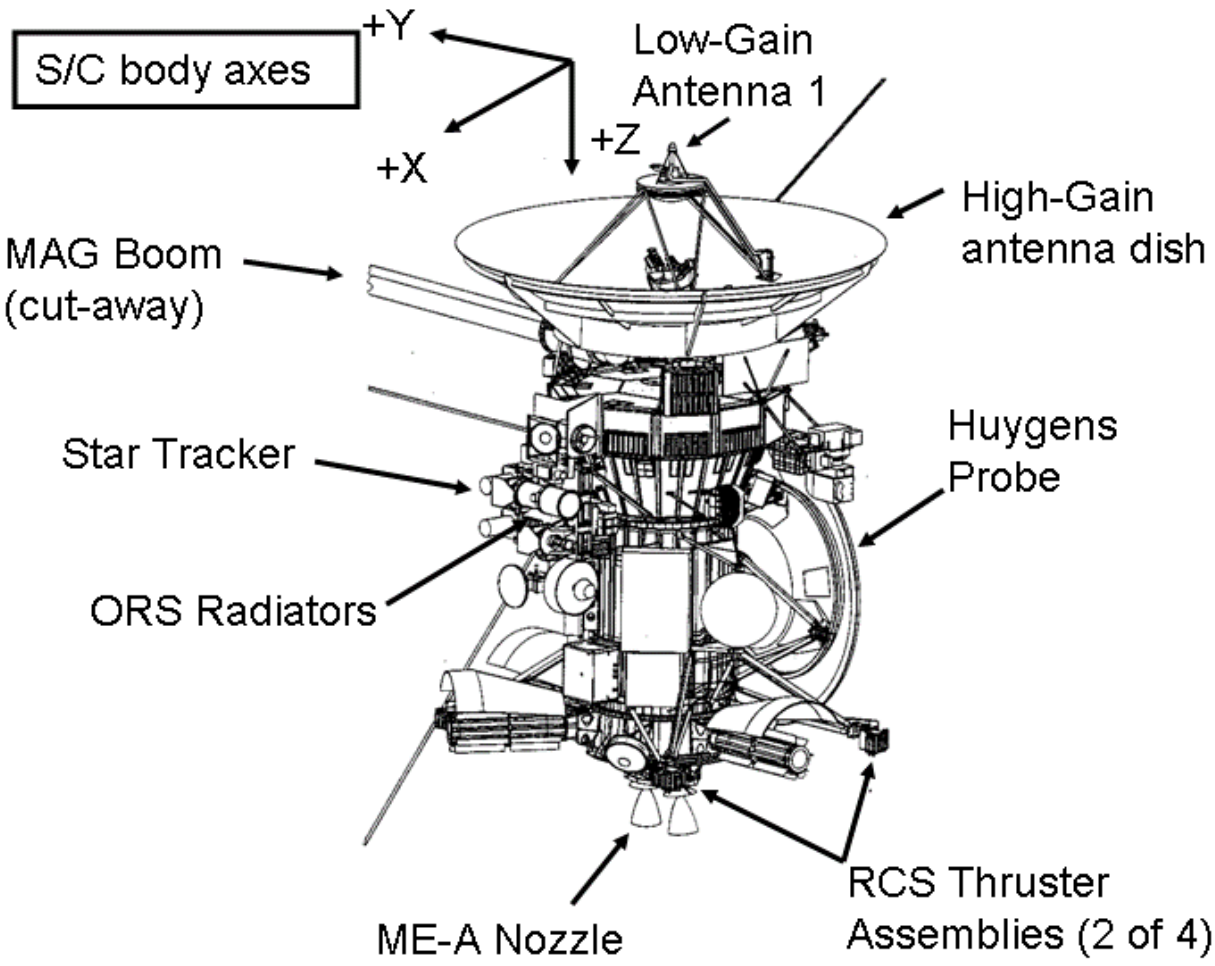

Figure 1. Cassini Cruise-phase Configuration (Both the multi-layered insulation and the main engine cover are omitted in this figure for clarity)

Cassini was equipped with an 11-meter long magnetometer boom and special sensors that enabled scientists to measure Saturn's magnetic field. Science goals of the Cassini magnetometer team included determining the interior structure and dynamics of Saturn via measuring the magnetic field to high precision. To achieve this goal, it is crucial

that Cassini's attitude -- its orientation in space -- be known to high accuracy. The peak background magnetic field at Saturn along Cassini's orbit is roughly 20,000 nano-Tesla (nT) and a 0.5 mrad angular error would contribute up to 10 nT noise to the vector magnetic field measurements. Most of the time, Cassini's onboard attitude knowledge is accurate to better than 0.5 mrad, but this requires good performance of the stellar reference unit and inertial reference unit. There are periods at Saturn when bright bodies enter the SRU field-of-view. During these periods, star identification (SID) is "suspended" for up to 5 hours until the spacecraft is quiescent and again has a clear star field. During SID suspends, onboard attitude estimates are propagated based solely on filtered angular rates from the body-fixed inertial reference unit. When the SRU comes back online at the end of the suspend, the first celestial attitude reference is called the "reacquisition" attitude. When this attitude is fed into the controller, a small jump in the attitude error occurs because of imperfect IRU-only propagation during the SID suspend. This jump is called the "reacquisition error."

Once transmitted to the ground, it is possible to adjust the IRU-only attitude time-history that occurred during the SID suspend. By taking the reacquisition error into account, the fidelity of the IRU-only attitude propagation can be improved. Early in the suspend, the IRU-only drift has not introduced much error. But later in the suspend, the adjustment can noticeably improve the estimated attitude and can be used by science teams in processing their data. Each of the 22 Grand Finale orbits had SID suspend periods that range from one to 5 hours. These occurred near the ring plane crossings just above Saturn's cloud tops and coincided with some of the most important magnetic field measurements of the entire mission. Without correcting for the IRU-only propagation errors, the magnetic field estimates are somewhat corrupted by spacecraft angular rotations errors. The high-fidelity attitude corrections can significantly reduce the corrupting influence of long periods of IRU-only propagation, allowing a much more precise Saturn-relative depiction of its detailed magnetic field.

III. Cassini IRU Calibrations

Cassini's attitude knowledge is based on SRU images which allow an absolute inertial reference. In between star tracker images, Cassini's attitude is propagated in flight software using IRU angular rate data. Cassini's IRUs consist of four Hemispheric Resonator Gyroscopes (HRGs). Three orthogonal HRGs are used as prime inertial sensors and one skew-oriented HRG is used as a parity checker. The HRG accurately senses rotational motion using the resonant vibrations of an axis-symmetric fused-silica shell (similar to a wine glass, which has no moving parts). Onboard attitude propagation involves incorporating IRU data via an extended Kalman-Bucy filter. As part of this filter, angular rate biases are actively estimated, and these bias estimates are always used when processing the HRG rate signals. Gyro scale factors and misalignments, which are especially important during a spacecraft slew, are fixed constants in the attitude estimation flight software. These scale factors and misalignments can also be estimated in the flight software -- by extending the number of states the Kalman filter is actively estimating. This is called a "gyro calibration" and can be initiated by a single ground command. This simple process allows ground controllers direct visibility of scale factor errors which can be monitored and trended to ensure robust attitude estimation. If the measured scale factors deviate too much from their values implemented in the FSW, mission operation team will consider an update of these values. If these scale factor errors were to grow too much, this would degrade onboard attitude knowledge especially during SID suspends. Such degradation could eventually lead to an autonomous fault protection response – including "safing" of the spacecraft – which would interrupt science gathering and scramble the ground controllers to try to return to normal operations.

As described by Brown[4], a Cassini IRU calibration is typically implemented in RWA control with slews of ±180º about each of the spacecraft body axes. Just prior to the first slew, the calibration command switches the Kalman filter to include 9 additional states: 3 gyro scale factor errors in S/C body frame and 6 misalignment parameters representing the physical IRU orientation relative to the FSW-specified IRU orientation. Burrough and Lee[5] express gyro-sensed rotation and angles in the form:

$$\vec{q}_{gyro} = \int \left(\vec{\omega}_{gyro} dt \right) + \vec{\delta}_{Angle} \tag{1}$$

$$\vec{\Omega}_{gyro} = \begin{bmatrix} 1+\varepsilon_X & 0 & 0 \\ 0 & 1+\varepsilon_Y & 0 \\ 0 & 0 & 1+\varepsilon_Z \end{bmatrix} \vec{\Omega}_{true} + \begin{bmatrix} 0 & \theta_{xy} & \theta_{xz} \\ \theta_{yx} & 0 & \theta_{yz} \\ \theta_{zx} & \theta_{zy} & 0 \end{bmatrix} \vec{\Omega}_{true} + \begin{bmatrix} b_X \\ b_Y \\ b_Z \end{bmatrix} + \vec{\Delta}_{Rate} \tag{2}$$

In Eq. 1, $\vec{q}_{gyro}$ is the measured spacecraft attitude vector due to the integrated time history of the IRU derived spacecraft body rates ($\vec{\omega}_{gyro}$) and the angle random walk of the IRU ($\vec{\eta}_{Angle}$). Furthermore, the accuracy of the measured spacecraft attitude, $\vec{q}_{gyro}$, has a finite resolution limited by the ~0.25μrad quantization of the data, though this is not reflected in Eq. 1. The measured spacecraft body rates, $\vec{\omega}_{gyro}$, is a combination of the true spacecraft body rates ($\vec{\omega}_{true}$) and errors introduced by the per axis scale factor errors (ε_i, $i \in \{X,Y,Z\}$), the sensing axes misalignments (q_{ij}, $i \neq j \in \{X,Y,Z\}$), the per axis rate bias (b_i, $i \in \{X,Y,Z\}$), and the rate random walk of the IRU, $\vec{\eta}_{Rate}$.

The prime gyro scale factor errors can be updated in the flight software, but does require a "patch" to replace the fixed constant with updated values. This has occurred during Cassini's mission[6], once prior to arrival at Saturn, and once during the mission at Saturn. The prime IRU was calibrated once per year, and the scale factor error estimates are depicted in Figure 2. The final prime gyro calibration (September 2016) estimated per-axis scale factor error to be: [2.2E-3, -5.5E-2, 2.15E-2] expressed as a percentage and in the spacecraft body frame (X, Y, Z). The Cassini scale factor errors have exhibited good stability since the last onboard update occurred in early February of 2007.

Measured Gyro Scale Factor Errors (relative to FSW)

SF Error (%)	7/13/02	2/28/03	3/12/04	2/9/05	2/10/06	2/27/07	3/5/08	3/4/09	2/25/10	2/11/11	2/8/12	2/7/13	1/17/14	12/18/14	12/13/15	9/16/16
X-axis	-5.00E-02	2.20E-02	3.80E-02	5.80E-02	6.80E-02	6.20E-03	1.40E-02	7.33E-03	8.78E-03	5.86E-03	1.18E-02	2.92E-02	1.75E-02	1.46E-02	8.44E-03	2.21E-03
Y-axis	1.96E-01	3.00E-03	3.70E-02	4.60E-02	7.90E-02	1.90E-03	-2.67E-04	-5.47E-03	-2.02E-02	-1.36E-02	-3.51E-02	-4.62E-02	-4.53E-02	-2.86E-02	-3.17E-02	-5.49E-02
Z-axis	4.90E-02	3.00E-02	4.60E-02	6.10E-02	6.50E-02	8.30E-03	5.48E-03	7.45E-03	8.12E-03	9.68E-03	1.31E-02	1.57E-03	1.09E-02	9.67E-03	1.00E-02	2.15E-02

Implemented in FSW A8.6.5 (and beyond)

New scale factor errors implemented in FSW A8.7.5 (and beyond)

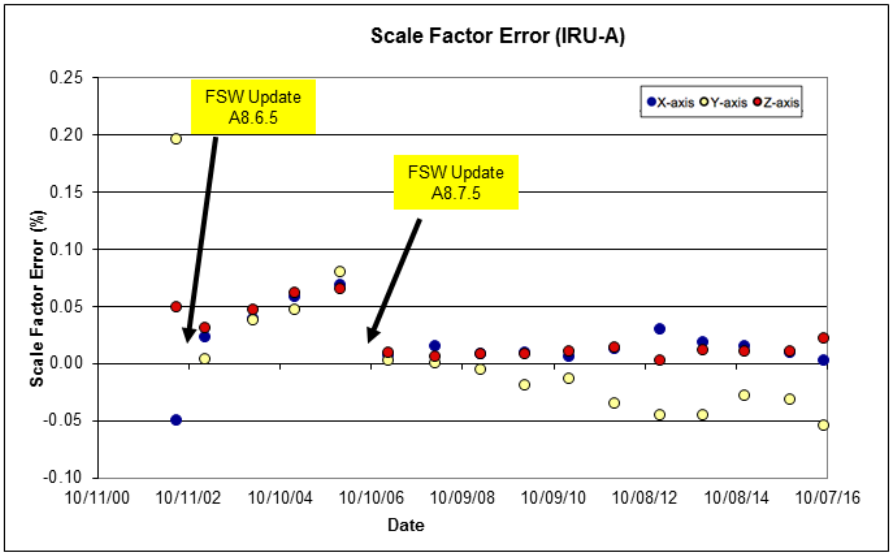

Figure 2. Prime Gyro Scale Factor Error Estimates. *Yearly calibration results are represented in the plot. Also shown are the two mission events where the onboard prime gyro scale factors were changed in the flight software. All percentage errors are relative to the most recent onboard update.*

IV. Correcting Attitude Errors Due To IRU Propagation Errors

Long SID suspends are a useful way to see the effects of gyro scale factor errors in flight telemetry. As an example, in the case of a 5-hour SID suspend during a long Z-axis rotation at 3.9 mrad/s, the 2.15E-2 percent scale factor error would produce a reacquisition attitude error correction (θ_{reacq}) of about 5 × 3600 × 3.9 × 2.15E-2 × .01 = 15 mrad (about 0.9º) about the Z-axis at the end of the SID suspend event. Although not observable in telemetry, the Z-axis error in this example most likely grew roughly linearly (with respect to total angular rotation) during the slew, from zero at the beginning of the SID suspend to 15 mrad at the end. During long Z-axis slews, scale factor error dominates the other sources and can be estimated in this case by: $\epsilon_z \approx \frac{\theta_{reacq}}{\theta slew}$ where θ_{reacq} is 15 mrad and θ_{slew} is about 70,200 mrad. The X and Y axes typically also exhibit some small reacquisition correction, due to misalignment error and/or random walk. The reacquisition error can be expressed as a vector in the S/C body frame $\vec{\theta}_{reacq}$. Following reacquisition, the attitude controller flight software commands rotational motion to null this 15 mrad error, so that at the end of the correction, the actual attitude (now that the SRU is once again providing a good celestial reference) finally is consistent with the commanded attitude.

Up until the beginning of the Grand Finale, the vast majority of long SID suspends (defined as longer than 4 hours) occurred during rolling downlink DSN tracks. Multiple revolution Z-axis rolls allowed the HGA to remain Earth-pointed while still collecting magnetometer and fields and particles science data. This allowed simultaneous data collection and playback. Figure 3 summarizes the Z-axis attitude correction for many long SID suspends at Saturn. The slow growth in the last few years is evidence of a small but continuing change in the physical prime IRU scale factor. The 20 mrad corrections at the very end reflect Grand Finale multi-revolution slews at a higher Z-axis slew rate than was normally used during the mission. The last few reacquisition corrections look bigger because of this bigger total slew angle. The cases with peaks less than 2 mrad slewed about X and Y but not the Z-axis.

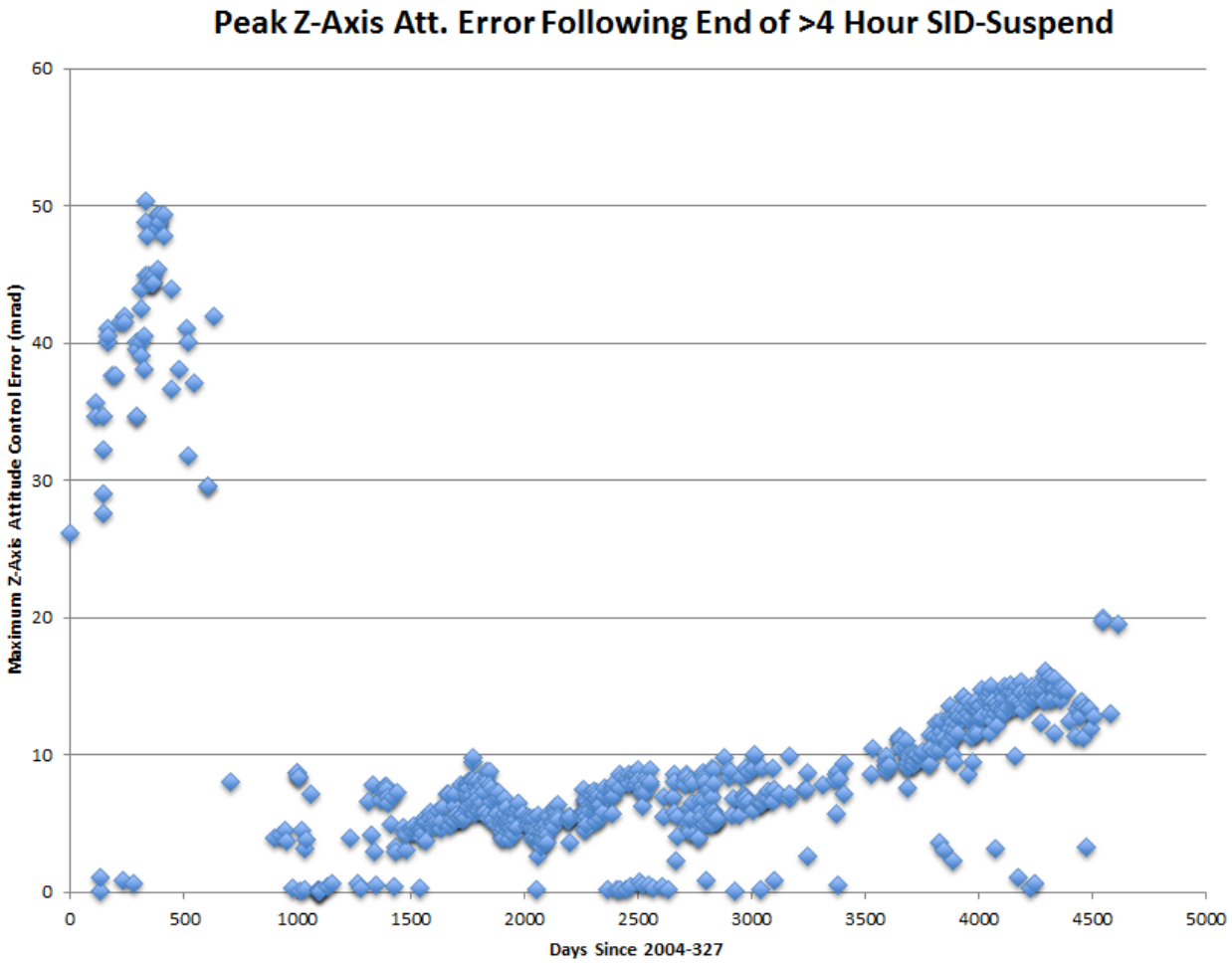

Figure 3. Z-Axis Reacquisition Error at end of long SID Suspends

Returning to our 15 mrad reacquisition example, during the period of the SID suspend, attitude telemetry is based on IRU-only data which would be in error by about 15 mrad at the end of the suspend. On the ground, the attitude telemetry could be "corrected" to incorporate the reacquisition correction, as expressed in Equation (1):

$$q_{inertial}^{corrected-body} = \quad qcorr_{uncorrected-body}^{corrected-body} \cdot \; qcorr_{inertial}^{uncorrected-body} \tag{3}$$

Where *q* is a 4-element attitude quaternion (a 3-vector and a scalar), *qcorr* is the attitude correction expressed as an error quaternion, and the "dot" operator is quaternion multiplication. The quaternion subscript is the "from" frame, and the superscript is the "to" frame. At the start of the suspend there is no correction and *qcorr* is an identity quaternion. *qcorr* grows throughout the suspend, in this case linearly with turn angle. The "uncorrected-body" is the telemetered quaternion representing Cassini's onboard attitude knowledge. If *qcorr* is correctly estimated, just as the SID suspend is ending, the "corrected-body" ideally matches the first post-suspend SRU-derived inertial reference – what we call the reacquisition attitude.

Equation (3) is actually a whole time-history of attitude estimates (spanning the suspend) and the goal is find a *qcorr* time-history that is based on reasonable estimates of IRU scale factor errors and yet approaches the reacquisition attitude correction (in this case, a Z-axis 15 mrad error) at the end of the suspend. The simplest case is when X and Y errors are negligible and the Z-axis correction is purely due to the scale factor error and grows linearly with rotation angle. The more general case, frequently seen in the Grand Finale, is when rotations occur about more than one axis during the SID suspend, and/or the suspend is long enough to introduce some random walk about each axis. How can *qcorr* be constructed in this more general case? Since there is only a single reacquisition correction, and there are both scale factor and random walk and other unknowns, there is likely no unique solution to this problem. However, the IRU scale factors errors are relatively well-known, based on IRU calibration results and, at least for the Z-axis, we have a lot of long SID suspend results that provide up-to-date information on the Z-axis scale factor errors.

To construct an attitude adjustment time-history -- *qcorr* in Equation (3) above – the spacecraft body rates during the SID suspend are used in conjunction with gyro scale factor error estimates. The one exception to this is when Cassini was quiescent throughout the SID suspend. There were 4 of these quiescent cases during the Grand Finale. For the cases where S/C slews did occur during the SID suspend, we begin by constructing "delta" attitude errors in the S/C body frame. Again $\vec{W}_{true}$ are the actual spacecraft body rates and ε_i are the estimated scale factor errors:

$$\Delta\vec{\theta}_{error(body)} = \vec{\Omega}_{true} \cdot \varepsilon_i \cdot \Delta t \tag{4}$$

delta attitude errors are then expressed in the J2000 inertial frame using the quaternion analog of the familiar direction-cosine matrix-vector equation:

$$\Delta\vec{\theta}_{error(J2000)} = q_{body}^{J2000} \cdot \Delta\vec{\theta}_{error(body)} \cdot q_{J2000}^{body} \tag{5}$$

The errors are then accumulated over the SID suspend period in the inertial frame. As part of this accumulation, an accumulated random walk error in each J2000 axis is added as an additional parameter. To simplify the analysis, misalignment errors are not included as separate error sources. This is reasonable especially based on data from long Z-axis SID suspends. Those results do not show any systematic error accumulation in the X or Y axes for long rotations about the Z-axis.

$$\vec{\theta}_{error(J2000)} = \sum[\Delta\vec{\theta}_{error(J2000)} + \Delta\vec{\theta}_{Random\_Walk(J2000)}] \tag{6}$$

$$\Delta\vec{\theta}_{Random\_Walk(J2000)} = \vec{\omega}_{Random\_Walk(J2000)} \cdot \Delta t \tag{7}$$

$\vec{\omega}_{Random\_Walk(J2000)}$ is the random walk rate, with vector components fixed in the J2000 inertial frame. This term acts as a single error vector that represents various physical, but small, terms. This term is needed when no reasonable set of gyro scale factor errors are able to match the reacquisition errors.

The *qcorr* time-history is estimated by choosing values for the scale factor errors (ε_i) and summing up the accumulated errors in the J2000 frame. A program does the Eq. 6 summation using S/C body rates, scale factor error estimates, and random walk estimates. At the time of SID reacquisition, the accumulated errors can be expressed in the S/C body frame:

$$\vec{\theta}_{accum\_error(body)} = q_{J2000}^{body} \cdot \vec{\theta}_{error(J2000)} \cdot q_{body}^{J2000} \tag{8}$$

The accumulated error at the end of the SID suspend ($\vec{\theta}_{accum\_error\_end(body)}$) can be compared against the reacquisition error $\vec{\theta}_{reacq}$. Through an iterative process of adjusting scale factor and random walk errors, a good fit can be found between $\vec{\theta}_{reacq}$ and $\vec{\theta}_{accum\_error\_end(body)}$. The best fits, although not unique or perfect solutions, provide better knowledge of the spacecraft attitude during the suspend than the uncorrected raw flight telemetry. This improved attitude time-history is then published to the Planetary Data System in the form of a C-Kernel[7] which is the standard format for attitude data developed by the Navigation Ancillary Information Facility. The Cassini magnetometer science team has used these C-Kernels in analyzing their data.

V. Attitude Correction Applied To Grand Finale SID Suspends

Magnetometer science data was captured during all 22 Grand Finale orbits, plus during the plunge on September 15, 2017. Each periapsis included an SID Suspend of 1 to 5 hours duration while Cassini was extremely close to Saturn and the rings. The Grand Finale began on April 16, 2017 during Saturn orbit (Rev) 271 and this paper focuses on reacquisition errors during Revs 272 through Rev 285 (July 25, 2017). The plunge into Saturn occurred during Rev 293. Table 1 summarizes the periapsis SID Suspends and the reacquisition errors noted in flight telemetry. The error correction process is the same when analyzing RCS or RWA control cases. The only difference is that after reacquisition, the RWA controller immediately corrects the reacquisition error while the RCS controller only does so if a bang-off-bang attitude control deadband is reached.

In Table 1, similar events have been grouped for clarity. Revs 272 and 285 are called Group A and are similar multi-revolution rotations about the S/C X-axis. These two periapses were dedicated to magnetometer science and the attitude reconstruction of these cases are especially important to the magnetometer team. Group B are the two multi-revolution Earth-pointed Z-axis rotations. Group C are the cases that stayed quiescent. The remainder in Group D each had rotations about all three body axes.

Note in Table 1 Group A that the reacquisition errors were considerably different, yet the long X-axis rotations were very similar. That seemed to be problematic – the body rates were almost identical and the physical scale factor errors had to be very close, so how could the reacquisitions be so different? The Z-axis reacquisition error, in particular, seemed puzzling because the errors were of different polarity! It turned out that small but significant differences in attitude during the two events led to significant variation in error accumulation in both the inertial and S/C body frames.

Group B contains the two multi-revolution slews almost completely about the Z-axis. The off-axis error magnitudes were -0.64, and -0.14 mrad (X-axis) and 0.36 and -0.02 mrad (Y-axis) after an SID suspend of 5 hours. This can be expressed as a "drift" angular rate between ±0.03 and ±0.15 mrad per hour. The long multi-revolution Z-axis slews produced Z-axis gyro scale factor errors, using the equation $\epsilon_z \approx \frac{\theta_{reacq}}{\theta slew}$, of 0.027% and 0.028% for the two cases. This is somewhat larger than the most recent gyro calibration estimate of 0.022%.

Group C is the four quiescent events where Cassini remained Earth-pointed during the ring plane crossings. The SID suspends for these cases were between 3 and 4 hours. The reacquisition magnitudes were between 0.5 and 0.85 mrad. This equates to a quiescent drift of between 0.17 to 0.25 mrad per hour. This compares well with an unplanned 9-hour quiescent drift in late 1998 that produced a correction of about 0.26 mrad per hour. Expressed in rad/s, the quiescent drift magnitudes were between 4.7E-8 rad/s and 6.9E-8 rad/s.

The attitude correction method for Group C was different than the other cases due to a quiescent spacecraft. With only a single reacquisition data point, a purely linear (with respect to time since suspend start) angular interpolation was chosen for these cases.

Table 1. SID Suspend Durations and Reacquisition Errors During the Grand Finale

		Reacquisition Correction		
Rev	SID Suspend Duration (H:MM:SS)	X-axis (mrad)	Y-axis (mrad)	Z-axis (mrad)
272	2:33:42	-1.93	0.89	-1.07
285	2:39:56	-0.61	0.06	1.03

Group A. These were multi-revolution rotations about the X-axis, preceded by a Z-axis turn. They were performed in RCS control to allow higher slew rates (4.5 mrad/s)

273	4:58:02	-0.65	-0.40	19.78
284	4:57:38	-0.14	-0.02	19.53

Group B. These were multi-revolution rotations about the X-Band boresight (very close to -Z-axis). They were at the highest slew rate of the mission (3.9 mrad/s) in RWA control.

274	3:04:32	0.40	0.35	0.06
275	3:04:32	0.5	0.22	-0.53
278	3:37:13	0.4	0.53	-0.53
280	3:37:13	0.36	0.63	0.05

Group C. These were quiescent Earth-pointed events.

276	2:43:12	-0.6	0.24	-0.11
277	1:42:17	0.2	-0.53	0.17
279	1:22:17	0.18	-0.27	-0.28
281	3:41:18	-0.17	1.10	-0.60
282	0:56:58	-0.05	0.02	0.63
283	2:07:27	0.82	-1.16	0.30

Group D. These had rotations about all three S/C body axes

Group D contains Revs 276, 277, 279, 281, 282, and 283. Each case slewed about all three S/C body axes, ranging from less than one up to 7 radians of total angular motion. A good example of the attitude correction process is Rev 283 where the reacquisition error was: [0.82, -1.16, 0.30] mrad. The SID suspend lasted 127 minutes. Figure 4 depicts the S/C body rates. Each plot below begins at the SID suspend start time and ends at reacquisition time.

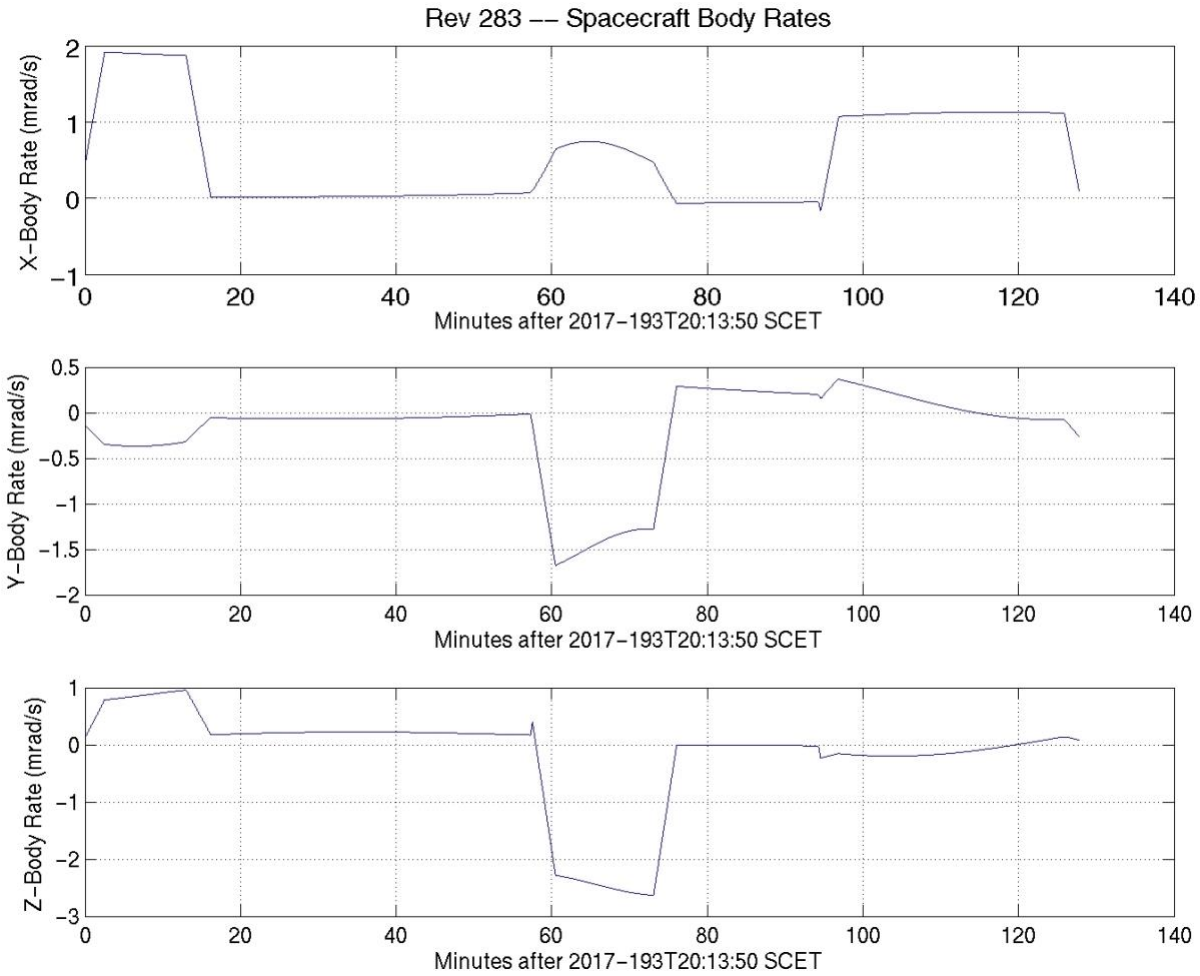

Figure 4. Spacecraft Body Rates During Rev 283 SID Suspend

Equation 6 is used with typical gyro scale factor errors and the S/C body rate time history for this SID suspend. Then the accumulated errors are compared against actual reacquisition errors. The process is repeated with small adjustments until a reasonably good match is achieved. Figure 5 shows the accumulated errors in the S/C body frame. The gyro scale factor errors (X, Y, Z) that produced the best match were: [-0.0356 0.026 -0.03]. All scale factor errors are expressed as a percentage and in S/C body frame. Adjusting the X-Axis scale factor error helped find a good match. In Figure 5, the dashed red lines are the actual reacquisition errors at the end of the suspend. A perfect fit would just touch each dashed red line at the end of the SID suspend.

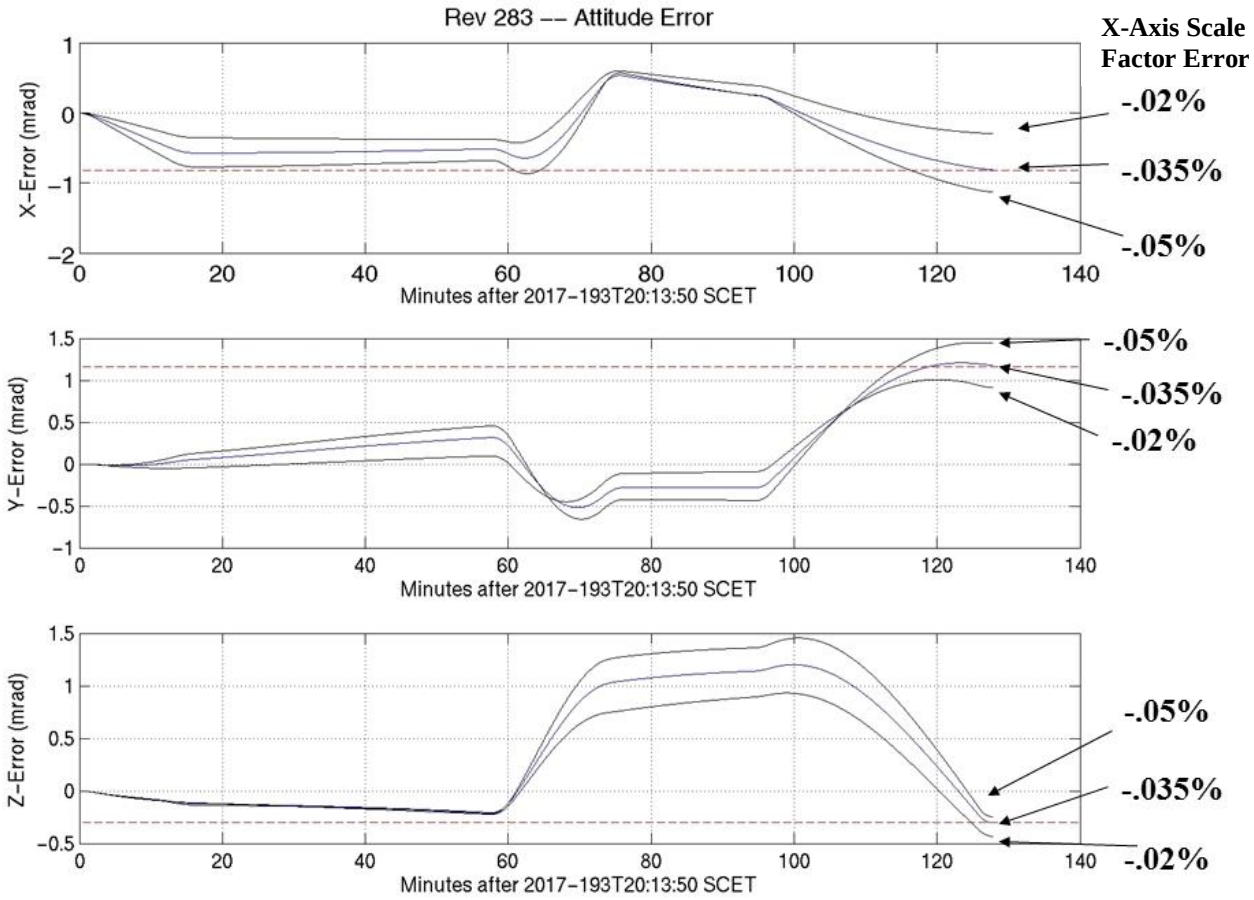

Figure 5. Rev 283 Accumulated Errors in Body Frame with X-Axis Scale Factor Error Adjustments. *The dashed red lines denote the actual reacquisition error at the end of the SID Suspend.*

The Group A cases from Table 1 are the two magnetometer multi-revolution slews about the S/C body X-axis. Figure 6 depicts the S/C body rates for these two cases during the SID suspends. Figure 7 shows the accumulated attitude errors for the best fit for these two cases. The fit parameters used in these cases is given in Table 2.

Table 2. Best Fit Scale Factor Errors and Random Walk Fixed Inertial Rate for Group A

		Best Fit Scale Factor Error			Best Fit Inertial Rate Error		
Rev	SID Suspend Duration (H:MM:SS)	X-Axis (%)	Y-Axis (%)	Z-Axis (%)	J2000X (rad/s)	J2000Y (rad/s)	J2000Z (rad/s)
272	2:33:42	-.0076	.026	-.029	-6.0E-8	0.0	-4.0E-8
285	2:39:56	-.0065	.026	-.03	2.0E-8	8.0E-8	1.0E-8

The fit accuracy of each case can be expressed as the magnitude of the difference between the accumulated attitude error vector and the reacquisition error vector:

$$\text{Fit Accuracy} = \left| \vec{\theta}_{accum\_error\_end(body)} - \vec{\theta}_{reacq} \right|$$

The magnitude of the Rev 285 reacquisition was 1.20 mrad. If the random walk was eliminated from the best fit, the accumulated attitude correction was 1.54 mrad. With the random walk, it was 1.21 (closely matching the 1.20 target). The random walk contributed about 1.54 – 1.21 = 0.33 mrad accumulated error (about 27% of the total). This is called the random walk contribution. It was not possible to find a good match without some random walk contribution. Table 3 summarizes the suspend durations, reacquisition error magnitude, fit accuracy, and random walk contribution.

Table 3. Reacquistion Magnitude, Fit Accuracy, and Random Walk Contribution in Group A

Rev	SID Suspend Duration (H:MM:SS)	Reacquisition Magnitude (mrad)	Fit Accuracy (mrad)	Random Walk Contribution (mrad)
272	2:33:42	2.375	0.058	0.24
285	2:39:56	1.196	0.027	0.33

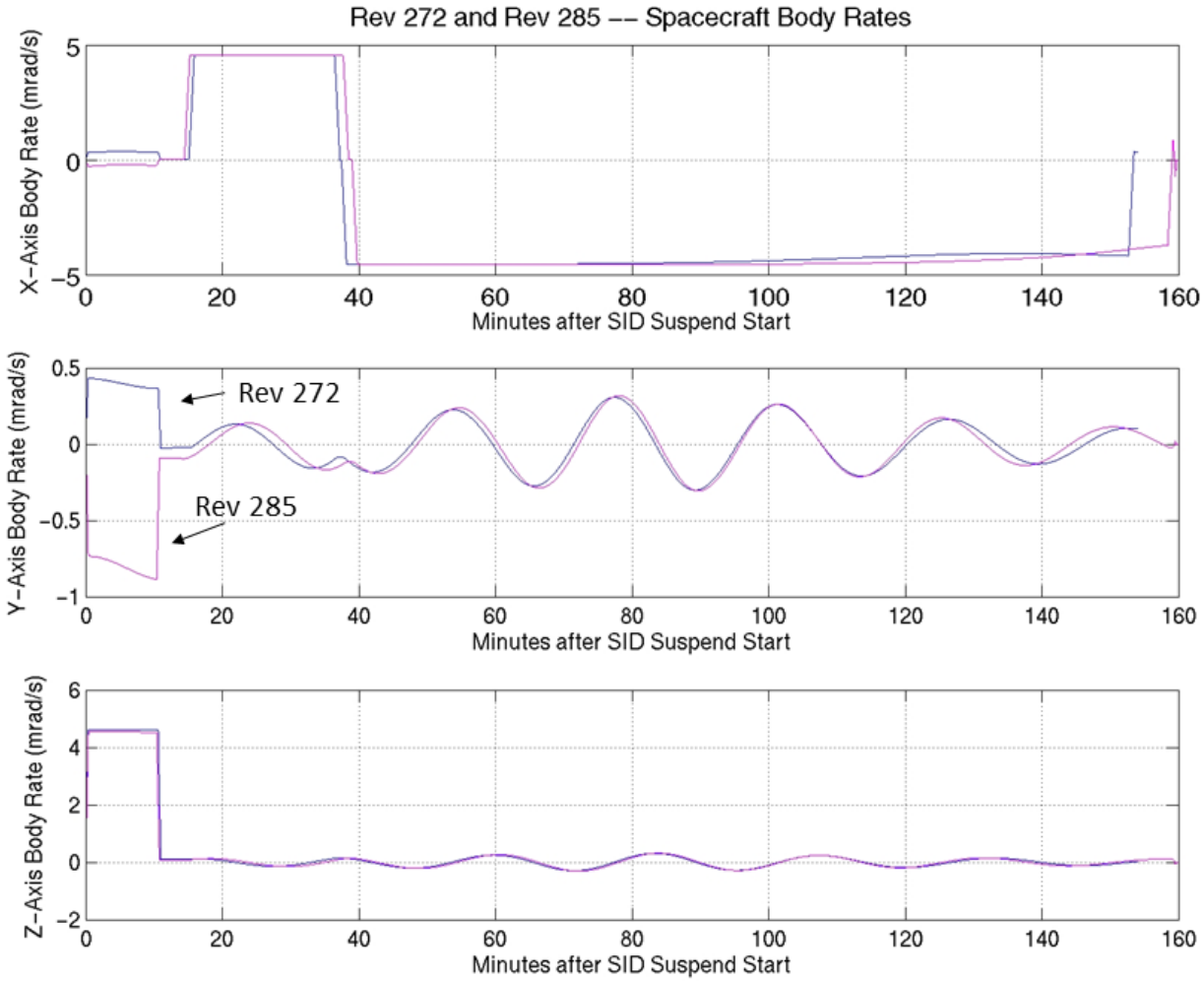

Figure 6. Body Rates during similar multi-revolution X-Axis magnetometer observations

Figure 7 depicts the accumulated attitude corrections for the best fits for the two Group A cases plotted in Figure 6. Small differences in the Y-axis slew led to much different accumulated attitude error by the end of each suspend. Note the oscillatory nature of the attitude error accumulation in the S/C body frame Y and Z axes. By examining the same accumulation in the inertial frame (Figure 8) it can be seen that the accumulated error oscillation in Figure 7 is really just an artifact of the rotating body frame.

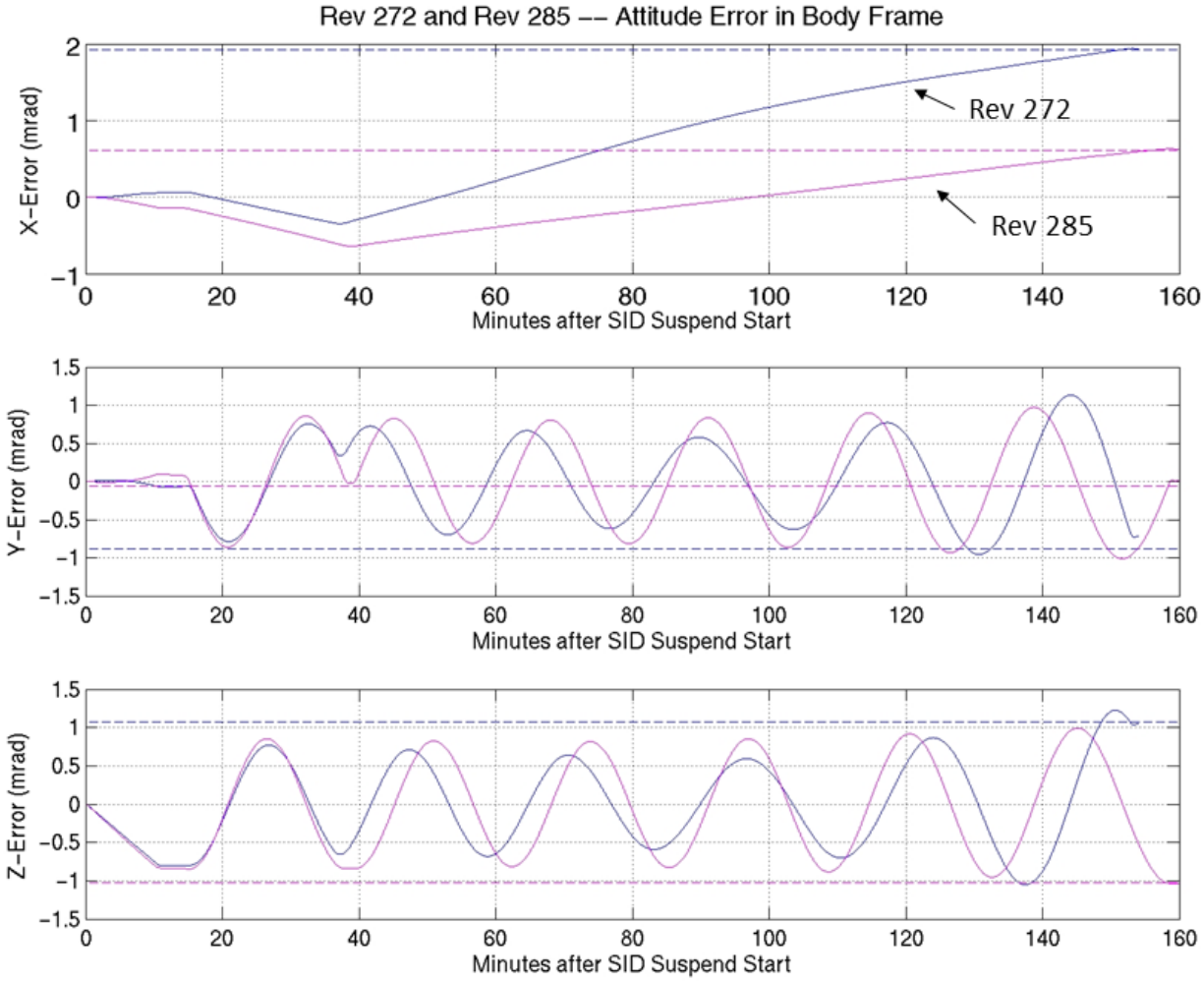

Figure 7. Best Fit Accumulated Error during similar multi-revolution X-Axis magnetometer observations

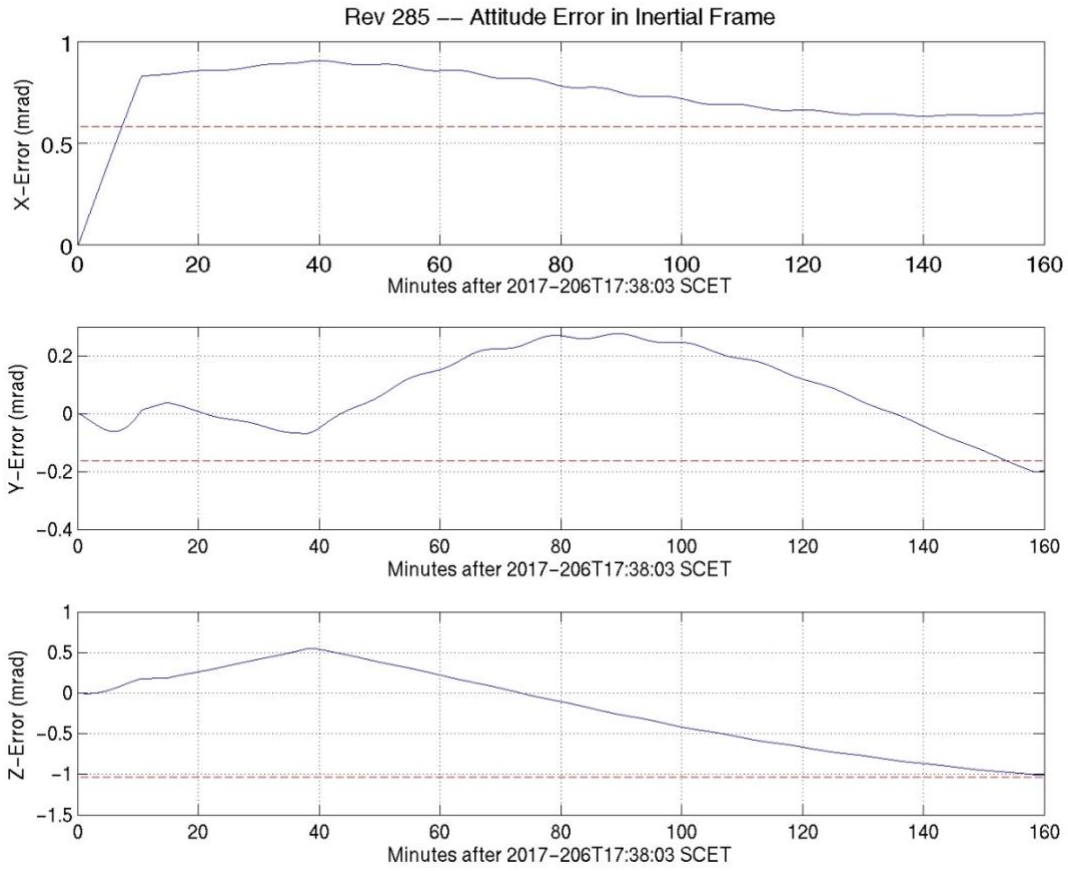

Figure 8. Best Fit Accumulated Error in the Inertial Frame for Rev 285.

Table 4 summarizes the suspend durations, best fit parameters, reacquisition magnitude, fit accuracy, and the random walk contribution for Group B. Table 5 summarizes the same information for Group D.

Table 4. Suspend Duration, Fit Parameters Reacquistion Magnitude, Best Fit Error, and Random Walk Contribution in Group B

		Best Fit Scale Factor Error			Best Fit Inertial Rate Error		
Rev	SID Suspend Duration (H:MM:SS)	X-Axis (%)	Y-Axis (%)	Z-Axis (%)	J2000X (rad/s)	J2000Y (rad/s)	J2000Z (rad/s)
273	4:58:02	-.003	.026	-.027	8.5E-9	6.6E-8	-5.0E-9
284	4:57:38	-.003	.026	-.028	9.3E-9	0	0

Rev	SID Suspend Duration (H:MM:SS)	Reacquisition Magnitude (mrad)	Fit Accuracy (mrad)	Random Walk Contribution (mrad)
273	3:53:09	19.789	0.014	1.08
284	4:57:38	19.532	0.023	0.02

Table 5. Suspend Duration, Fit Parameters, Reacquistion Magnitude, Best Fit Error, and Random Walk Contribution in Group D

		Best Fit Scale Factor Error			Best Fit Inertial Rate Error		
Rev	SID Suspend Duration (H:MM:SS)	X-Axis (%)	Y-Axis (%)	Z-Axis (%)	J2000X (rad/s)	J2000Y (rad/s)	J2000Z (rad/s)
276	2:43:12	-.032	.027	-.03	-2.5E-8	-1.5E-9	-3.5E-9
277	1:42:17	-.003	.026	-.03	-8.0E-9	-3.0E-8	2.0E-8
279	1:22:17	-.003	.026	-.03	1.0E-7	-1.0E-8	0
281	3:41:18	-.003	.026	-.03	0	2.7E-8	6.6E-8
282	0:56:58	-.0066	.026	-.03	-9.0E-8	2.0E-8	5.0E-8
283	2:07:27	-.0356	.026	-.03	0	1.2E-8	0

Rev	SID Suspend Duration (H:MM:SS)	Reacquisition Magnitude (mrad)	Fit Accuracy (mrad)	Random Walk Contribution (mrad)
276	2:43:12	0.702	0.025	0.02
277	1:42:17	0.592	0.021	0.19
279	1:22:17	0.424	0.037	0.26
281	3:41:18	1.261	0.008	0.25
282	0:56:58	0.628	0.095	0.04
283	2:07:27	1.454	0.021	0.03

VI. Saturn Magnetic Field Measurements with Corrected Attitude Estimation

The attitude correction process was performed on each of the Grand Finale cases and the best fits were passed on to the magnetometer team in the form of attitude C-Kernels. The magnetometer team evaluated both the uncorrected reconstructed C-Kernels (based directly on telemetry) and the corrected reconstruction C-Kernels. An example of how they compare is given in Figure 9. The Saturn magnetic field should be a Saturn-relative field that is independent of Cassini motion or orientation in space. In Figure 9, the upper plot has a number of significant oscillations in all three axes. The scientists refer to these artifacts as "spin tones" because they are likely caused by errors in Cassini's attitude during the multi-revolution X-axis spin during the Rev 272 SID suspend. The upper plot is based on the uncorrected reconstructed C-Kernel delivered soon after the data was played back. As it became clear that the magnetic field measurements were very sensitive to accurate Cassini orientation, the correction process outlined in this paper was developed. Corrected C-Kernels were generated by the author and used by the magnetometer teams. The resulting analysis is summarized in the lower plot in Figure 9. That plot shows the spin tones are mostly eliminated by using the corrected C-Kernel. The two peaks that remain are real Saturn-relative magnetic field signatures generated by Saturn and seen in all the Grand Finale periapses. The magnetometer team has expressed great enthusiasm in their magnetic field investigations based on the corrected C-Kernels.

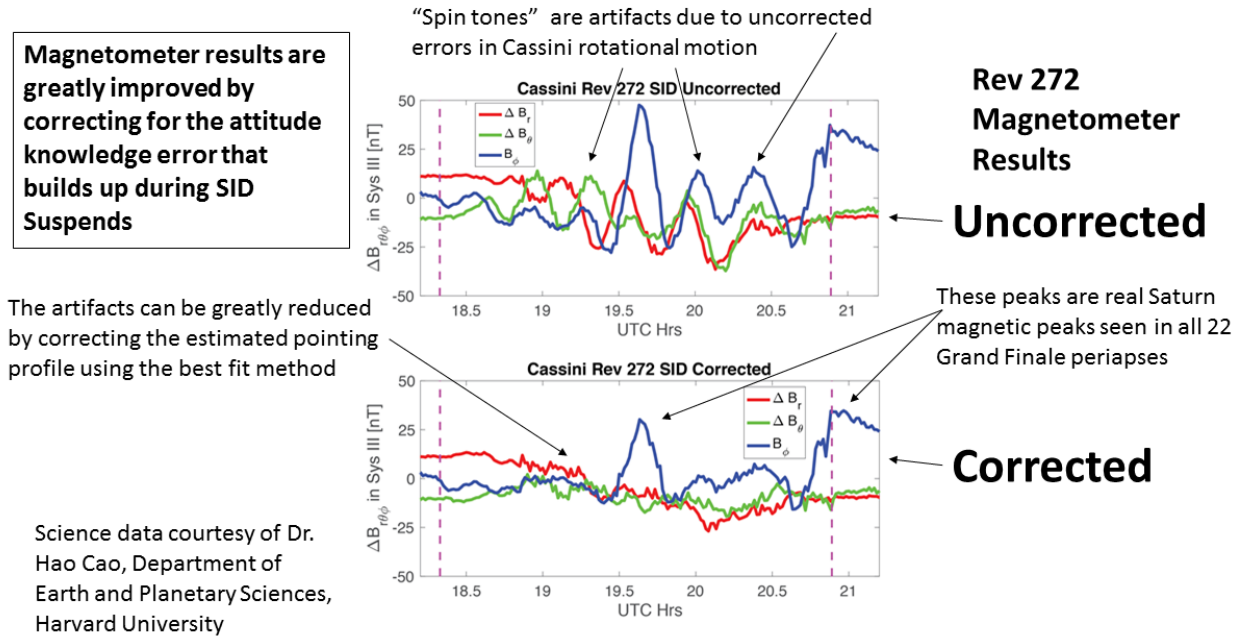

Figure 9. Rev 272 Magnetometer Results

VII. Conclusions

The Cassini Grand Finale produced unique scientific results including magnetometer measurements that may rewrite the story of Saturn's magnetic field. Some of the most unique magnetometer measurements occurred near periapses which coincided with SID suspends from one to five hours in duration. Gyro-only propagation during these suspends introduced attitude knowledge errors that were only corrected at the end when the star tracker came back online. These reacquisition corrections can be used to improve on the uncorrected raw spacecraft attitude telemetry throughout each lengthy SID suspend. When carefully fitted, the corrected attitude virtually matches the first celestial reference obtained after the star tracker comes back online. The corrected attitude time-history is a better approximation of the true spacecraft attitude throughout the entire SID suspend. The corrected attitude is put into

standard NAIF C-Kernel format and published so that the Cassini science teams – the magnetometer team in particular – can use them to improve the fidelity of their science results. The magnetometer team has processed the corrected C-Kernels with their raw measurements and demonstrated that a lot of noise and spacecraft "spin tone" artifacts are removed from their measurements, providing a much better picture of Saturn's true magnetic field.

VIII. Acknowledgments

The research described in this paper was carried out at the Jet Propulsion Laboratory, California Institute of Technology, under contract with the National Aeronautics and Space Administration. Reference to any specific commercial product, process, or service by trade name, trademark, manufacturer, or otherwise, does not constitute or imply its endorsement by the United States Government or the Jet Propulsion Laboratory, California Institute of Technology.

The author would like to acknowledge the prior work of Todd S. Brown, Allan Y. Lee, and Emily Burrough Pilinski, in analyzing and reporting the results of the Cassini IRU behavior. I also want to acknowledge the Cassini Magnetometer team, including Dr. Hao Cao, Department of Earth and Planetary Sciences, Harvard University, Dr. Krishan Khurana, Department of Earth and Space Sciences, UCLA, and Dr. Michele K. Dougherty FRS, Professor of Space Physics, Imperial College, London. Dr. Cao graciously provided Figure 9 of this paper as well as valuable technical explanations. Furthermore, I would also like to thank the Cassini AACS team, including, David Bates, Joan Stupid, Luis Andrade, and Eric Wang for their feedback and contributions to this analysis. I also want to thank the Cassini spacecraft manager, Julie L. Webster, for her support and guidance.

IX. References

[1] Burk, T., "Cassini at Saturn Proximal Orbits – Attitude Control Challenges," Paper AIAA-2013-4710, *Proceedings of the AIAA Guidance, Navigation, and Control Conference*, Boston, MA, Aug. 19-22, 2013.

[2] Sung, T., "Attitude Control Subsystem Performance of the Cassini Spacecraft During Proximal Ring Plane Crossings between Saturn and the Innermost D-Ring," *SciTech 2018 AIAA Guidance, Navigation, and Control Conference*, Kissimmee, FL, Jan. 8-12, 2018 (to be published)

[3] Stupik, J., "Mission Summary of Cassini Spacecraft Guidance and Control Hardware Health and Performance," *SciTech 2018 AIAA Guidance, Navigation, and Control Conference*, Kissimmee, FL, Jan. 8-12, 2018 (to be published)

[4] Brown, T. S., "In-Flight Performance of the Cassini Hemispherical Quartz Resonator Gyro Inertial Reference Units," Paper AIAA-2013-4630, *AIAA Guidance, Navigation, and Control Conference*, Boston, MA, Aug. 19-22, 2013.

[5] Burrough, E. L. and Lee, A. Y., "In-flight Characterization of Cassini Inertial Reference Units," Paper AIAA-2007-6340, *Proceedings of the AIAA Guidance, Navigation, and Control Conference*, Hilton Head, South Carolina, August 20-23, 2007.

[6] Lee, A. Y. and Hanover, G., "Cassini Spacecraft Attitude Control System Flight Performance," Paper AIAA-2005-6269, *Proceedings of the AIAA Guidance, Navigation, and Control Conference*, San Francisco, California, August 15-18, 2005.

[7] Acton, C., et al, "Extending NASA's Spice Ancillary Information System to Meet Future Mission Needs," *Proceedings of SpaceOps 2002 Conference*, October 8-11, 2002.